A COMPACT ELECTRON SPECTROMETER FOR AN LWFA*

A.H. Lumpkin**, R. Crowell, Y. Li, and K. Nemeth
Argonne Accelerator Institute, Argonne National Laboratory, Argonne, IL 60439, U.S.A

Abstract

The use of a laser wakefield accelerator (LWFA) beam as a driver for a compact free-electron laser (FEL) has been proposed recently. A project is underway at Argonne National Laboratory (ANL) to operate an LWFA in the bubble regime and to use the quasi-monoenergetic electron beam as a driver for a 3-m-long undulator for generation of sub-ps UV radiation. The Terawatt Ultrafast High Field Facility (TUHFF) in the Chemistry Division provides the 20-TW peak power laser. A compact electron spectrometer whose initial fields of 0.45 T provide energy coverage of 30-200 MeV has been selected to characterize the electron beams. The system is based on the Ecole Polytechnique design used for their LWFA and incorporates the 5-cm-long permanent magnet dipole, the LANEX scintillator screen located at the dispersive plane, a Roper Scientific 16-bit MCP-intensified CCD camera, and a Bergoz ICT for complementary charge measurements. Test results on the magnets, the 16-bit camera, and the ICT will be described, and initial electron beam data will be presented as available. Other challenges will also be addressed.

INTRODUCTION

One of the challenges of the laser wakefield accelerator (LWFA) project is generation of robust, quasi-monoenergetic electron beams. At the AAC06 Workshop a number of laboratories reported observation of such beams ranging in energies from 10s of MeV to 1 GeV with charges ranging from 10 s to 100 s of pC [1]. The Chemistry Division is currently using and developing an LWFA within their Terawatt Ultrafast High Field Facility (TUHFF) [2]. Although pulsed radiolysis chemistry experiments are the primary objective, an initiative to demonstrate an LWFA operating in the bubble regime [3] with quasi-monoenergetic beams is being driven by Strategic LDRD funds. A long-range goal of this project is to use the beam to drive an undulator for generation of ultrafast spontaneous radiation. Other laboratories have targeted the possible driving of a free-electron laser (FEL) [4]. As part of the present ANL project, characterization of the electron beams generated is a critical aspect. Towards this end an electron beam spectrometer is needed to measure the electron beam spectrum to look for the energy peak and energy spread. This is in addition to a basic charge measurement and a beam divergence measurement. The compact spectrometer design is based on that reported by Glinec et al. [5].

*Work supported by the U.S. Department of Energy, Office of Science, Office of Basic Energy Sciences, under Contract No. DE-AC02-06CH11357.
**lumpkin@aps.anl.gov

EXPERIMENTAL BACKGROUND

The 20-TW laser at TUHFF consists of a three-stage chirped-pulse amplified Ti:Sapphire laser system running at 10 Hz. The 15-fs (FWHM) seed pulse train from the oscillator is stretched to 440 ps in a double-pass single grating stretcher, and then a Pockels cell pulse picker is used to lower the repetition rate to 10 Hz. The beam passes through a three-stage amplifier and then is directed into a two-grating pulse compressor resulting in a 600-mJ, 30-fs (FWHM) pulse of 20 TW. A schematic is shown in Fig. 1. A more detailed description of the laser system can be found elsewhere [6]. The compressed laser beam is then directed into the interaction chamber and focused to about 30 µm size onto the 1.2-mm-diameter supersonic He gas jet. Electron pulses of relativistic energies are generated and pass through a rotating Cu disk that blocks the laser beam, but transmits the electrons to a sample or the electron spectrometer or other diagnostics.

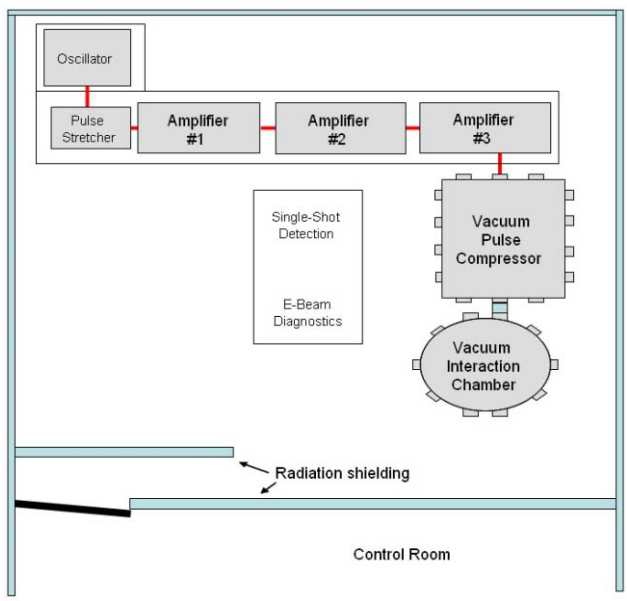

Figure 1: Schematic of the TUHFF with the Ti:Sapphire oscillator, pulse stretcher, three amplifiers, pulse compressor, and the interaction chamber.

Compact Electron Spectrometer

The major components of a compact electron spectrometer based on the Ecole Polytechnique University LOA design [3,5] are the permanent magnet dipole; the scintillator screen at the dispersive plane; the 16-bit CCD camera with optics, which views the screen; and an integrating current transformer (ICT) for complementary charge measurements.

Permanent Magnet Dipole: The two NdFeB magnets are 5 cm long by 2.5 cm wide by 1.2 cm thick. Magnet characterization was performed by the APS Magnetic

Devices Group in their ID magnet measurement facility. Both magnets were characterized and their reference files generated. This was requested in case there is subsequent radiation damage to the magnets from energetic electrons in the LWFA. A collimator may be appropriate before the magnets. The one magnet field strength vs. z plot was determined. A gap was selected to replicate the 0.45 T values of the LOA magnets [4]. That gap is 12 mm for two magnets, although there is an end effect that may reduce the effective dispersion. This provides coverage for 20-, 50-, 100-, and 200-MeV electrons with varying dispersion resulting in energy resolutions of 6, 14, 27, and 53%, respectively [5]. In addition, effective energy resolution can be limited by the natural divergence and beam size at the scintillator screen.

With the completion of the magnet holder assembly, the two magnets were positioned with a 12-mm gap, and the combined fields in this configuration were measured in the APS magnet measurement facility. The plot of field strength versus z is shown in Fig. 2. The total field is about 0.46 T as expected with some end effects again that will reduce the effective dispersion 5-10%.

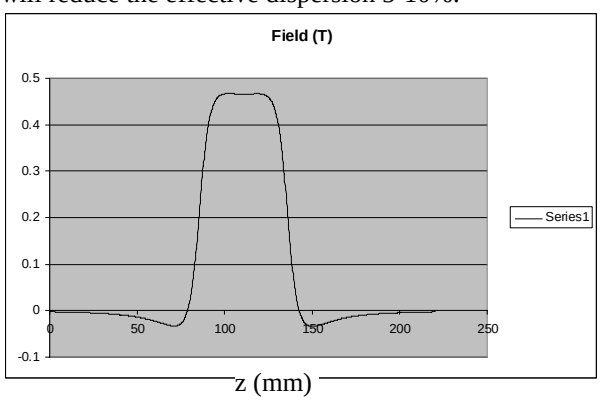

Figure 2: Map of the field strength along the z axis for two 5-cm long magnets with a 12-mm gap. The horizontal axis is in mm (courtesy of Isaac Vasserman, APS).

LANEX Scintillator: Extensive tests have been done previously with the Kodak x-ray screen called LANEX [4]. This is essentially a Gd_2O_2S:Tb inorganic scintillator with efficient conversion of both x-ray and electron incident energies. It has been reported to give similar energy absorption per electron for electron energies from 10 MeV to 500 MeV so it is a good candidate for the converter screen in the spectrometer [4]. These emit in the blue-green with a strong component at 548 nm, which is a good wavelength match to CCD quantum efficiency curves.

16-bit ICCD Camera: A Roper Scientific 16-bit camera was selected for use as the readout of the energy information displayed on the screen. The camera is Peltier-cooled and has a 1024 × 1024 array with 13-µm-square pixels. It has a PCI card that includes the digitizers to provide 16-bit deep images. The microchannel plate (MCP) intensifier tube is of a high quality with 6-µm-diameter channels for the 18-mm-diameter tube. There is a Roper software package loadable on the PC to display and minimally process images. Other programs are used for profile analysis.

The ICCD was taken to the APS S35 optics lab for calibration and resolution tests. We also simulated a working configuration of the PCs being 100 ft away in another lab from the camera control unit and camera head. This is basically how it would run in the LWFA lab.

The camera was mounted on a rail with carriers so the 105-mm F-mount Nikon zoom lens could be used at different working distances. The calibration lab has a platform holding a filter wheel that includes a back-illuminated 15-µm diameter pinhole as a resolution test object and a grid pattern for spatial calibrations. The platform can be moved in three dimensions for centering the source or scanning the field of view and for precise z-motion relative to the camera lens distance to optimize focus. A photograph of the setup is shown in Fig. 3.

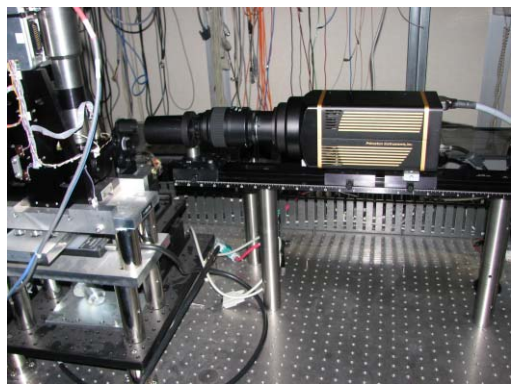

Figure 3: Photograph of the ICCD camera on the S35 optical calibration table. Calibration factors and resolution tests were done for various lens distances.

The tests were initially done at working distances of 14 cm, 17.3 cm, and 29 cm. The grid pattern was used to obtain the calibration factor in each case. A bright square, 10 mm on each side, was used as the main reference. Fine features in the pattern were used for initial focus adjustments. We then selected the pinhole source and scanned the z direction over several mm. An example of the preliminary depth-of-focus results for a working distance of 17.3 cm is shown in Fig. 4, where the FWHM resolution is 2.5 ch or 50 µm. These data show that for this lens setting, resolution can be degraded if the z position is off by 3 mm from the center of the focus curve. A separate Air Force line-pair pattern was used as well at this working distance.

Additional working distances were used at 40, 50, 60, and 70 cm, but the resolution test was not done because we had consistently obtained the 2.5-ch FWHM result, just with different calibration factors. The calibration factors and expected field-of view (FOV) are shown in Table 1. With our LWFA geometry we will view the scintillator back at the 40-70 cm working distance with the camera located outside the chamber looking through the port. A pumpout port was moved, and we installed a window in the port more directly downstream of the

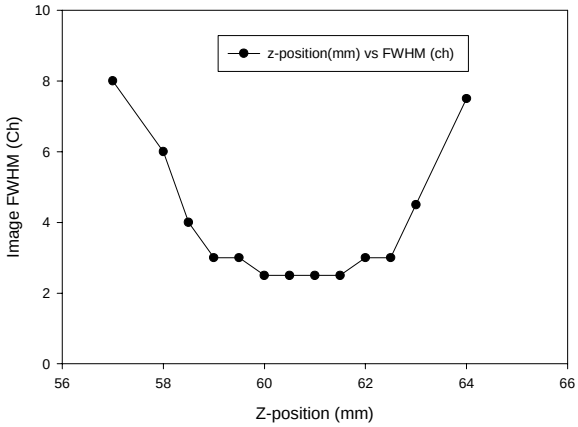

Figure 4: Depth-of-focus scan for a working distance of 17.3 cm for the 105-mm lens. The 2.5 ch (FWHM) resolution would be 50 μm for this calibration factor.

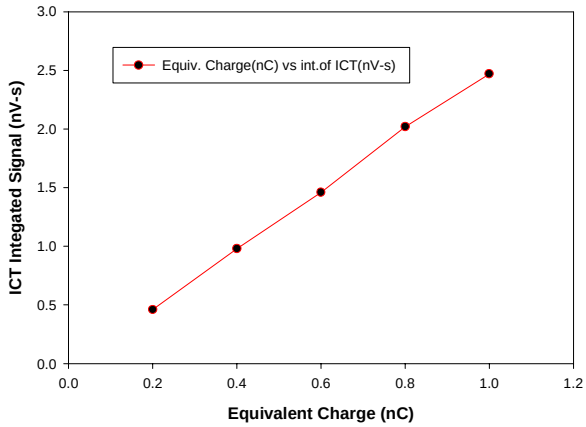

Figure 5: Test results for the Bergoz ICT showing the equivalent charge input and the signal response output (integrated) of the ICT in nV·s.

interaction zone for viewing images on the back of the scintillator.

Table 1: Summary of the Calibration Factors and FOVs for 105-mm Zoom Lens Working Distances

Working Distance (cm)	Calibration Factor (μm/pixel)	FOV (cm)
14.0	13.7	1.4
17.3	19.6	2.0
29.0	36.9	3.8
40.0	50.0	5.1
50.0	62.5	6.3
60.0	74.0	7.6
70.0	89.3	9.1

ICT: A Bergoz ICT is expected to be used in vacuum with a return loop added to provide complementary charge measurements (although the LOA experiments indicated background issues and gave a large error bar on absolute measurements [5]). Initially the existing Faraday cup will be used for experiments.

The ICT was tested using an HP 8114A pulse generator. With the pulse width set at 10 ns, one could set the level to 1 V to have 10 nV·s injected on a wire passing through the center of the ICT. This corresponded to 0.2 nC into a 50-ohm test load. The voltage level was adjusted to vary the injected charge, and the results are shown in Fig. 5. The integrated ICT signal output was determined using the Agilent Infinium 54854A oscilloscope operating in the "integrate mode." The scope trace had ~16 mV peak with 30 ns (FWHM) for the 0.2-nC input. This means that a low-noise environment is needed for seeing 10 s of pC pulses in the LWFA.

Proposed Layout

The LWFA main chamber is ~1.3 m in diameter; however the location of the gas jet nozzle is on one side of a 30-cm-diameter pumpout port centered in the chamber floor and is ~35 cm from the chamber wall. This latter distance is a constraint for installing hardware downstream of the nozzle. First the rotating copper disk is put in, which blocks the intense laser beam and transmits generated electrons. A 6.2-cm lead collimator with a 10-mm-diameter hole at beam centerline may be needed. The magnets are 5 cm long with a 12-mm gap, and the LANEX screen is positioned 17 cm downstream from the entrance edge of the magnets. The LANEX is fronted by a thin Aluminum foil to block laser light leakage if there is any. The screen is about 10 cm wide by 2.5 cm high. The ICCD camera with lens has been positioned at the port to view the back of the LANEX at a working distance TBD, but on the order of 40-70 cm to give the FOV in energy. Two mirrors in the optical path outside the chamber redirect the scintillator light to the lead-shielded camera location. The camera is mounted on a Newport rail supported by a small optical breadboard. The small Faraday cup will initially be positioned for charge measurements. Installation is nearly completed except for final alignment and electrical signal connections.

An initial experiment will be done with no magnets to look for low divergence beams at the LANEX with the FC and camera behind the LANEX. If there is a low-divergence electron beam, there should be quasi-monoenergetic beam as well based on our interpretation of the literature [3]. Also, we can check for the calculated beam size asymmetry with the larger size in the direction of the incident laser polarization as reported by Nemeth et al. [7]. Since the polarization is horizontal in the ANL LWFA, we may need to rotate the spectrometer plane. With enough charge and signal, the complementary OTR experiments from the disk downstream side and a thin foil could be pursued. If there is any microbunching of the beam at blue-shifted wavelengths of the fundamental laser wavelength, the signature should be confirmable with a visible light spectrometer.

EXPERIMENTAL AND ANALYTICAL RESULTS

As mentioned in the previous section, the ANL results are only in an early phase although prompt electrons were generated and used for photolysis experiments in the past

[2]. Simulations were done at ANL using the code VORPAL to evaluate the expected performance of the present LWFA [7,8]. Beam energies of the order of 100 MeV are expected with a plasma density of ~5 × 10^{18} e/cm^3 and the properly focused laser spot (10^{18} W/cm^2) at the gas jet. As shown in Fig. 6, the e-beam should actually exhibit some longitudinal structure which is analogous to SASE-induced microbunching in an FEL. In this case it is the structure impressed by the co-propagating laser fields as the trapped electrons are accelerated though the plasma. Coherent OTR would be generated when such beams transit a dielectric boundary. Such an effect has been reported in the last year by Glinec et al. [9]. In another development, the use of colliding laser beams to produce a more controlled injection of electrons into the LWFA process has resulted in tunable beam energies and more reproducible performance as reported by J. Faure et al. [10]. The longer range goal to use an LWFA beam to drive undulator radiation is schematically shown in Fig. 7. As techniques improve one can expect continued progress in beam quality in regards to energy, energy spread, charge, and emittance. It is difficult to predict the evolution time at this point, but generation of 10-GeV beam by the time of ACC08 is the community target [1] with 1 GeV already demonstrated [11].

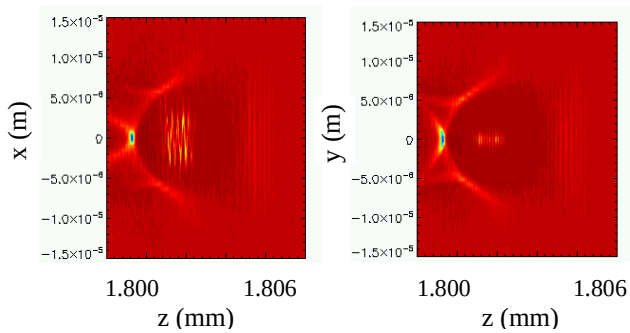

Figure 6: Simulation of the LWFA bubble regime for x-z polarization plane (left) and y-z plane (right) displays of microbunching.

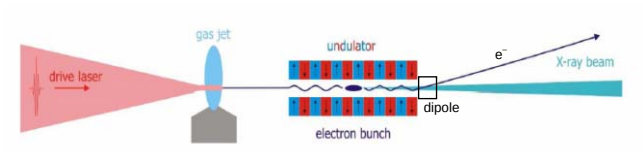

Figure 7: A schematic of the LWFA beam generating spontaneous emission radiation in an undulator.

SUMMARY

In summary, the ANL LWFA project is on the verge of generating electrons again, and a compact electron spectrometer has been installed to look for quasi-monoenergetic beam behavior. The challenge of generating enough charge (100s of pC) with low emittance and energy spread will have to be met before serious work with an undulator would be feasible. The initial ultrafast pulse lengths of the laser can be transferred to the trapped electrons in the bubble regime so generation of short-pulse radiation from an undulator is feasible.

ACKNOWLEDGMENTS

The authors acknowledge the support of R.Gerig and K.-J Kim of the Argonne Accelerator Institute and the assistance of I. Vasserman, B. Yang, J. Power, A. Brill, and T. Pietryla on component testing and of S. Chemerisov for LWFA interaction chamber setup.

REFERENCES

[1] Proceedings of the AAC06, M. Conde and C. Eyberger (Eds.), July 15-22, 2006, Lake Geneva, WI, AIP Conf. Proc. 877 (2006) and references therein.
[2] D.A. Oulianov et al., "Ultrafast Pulse Radiolysis Using a Terawatt Laser Wakefield Accelerator," submitted to J. Appl. Phys. (2006).
[3] V. Malka et al., "Monoenergetic Electron Beam Optimization in the Bubble Regime," Phys. of Plasmas **12**, 056702 (2005).
[4] C.B. Schroeder et al., "Design of an XUV FEL Driven by the Laser Plasma Accelerator at the LBNL LOASIS Facility," Proc. of FEL06, Berlin, Germany, pp. 455-458 (2006); http://www.jacow.org.
[5] Y. Glinec et al., "Broadrange Single Shot Electron Spectrometer," Ecole Polytechnique report dated July 6, 2006.
[6] R.A. Crowell et al., Radiat. Phys. Chem. **70**, 501 (2004).
[7] Karoly Nemeth et al., "Laser driven coherent betatron oscillation in a laser-wakefield cavity," submitted to PRL 2007.
[8] Yuelin Li, private communication, February 14, 2007.
[9] Y. Glinec et al., "Observation of Fine Structures in Laser-Driven Electron Beams Using Coherent Transition Radiation," Phys. Rev. Lett. **98**(19), 194801 (May 2007).
[10] J. Faure et al., Nature **444**, 737 (2006).
[11] W. Leemans et al., "GeV electron beams from a centimeter-scale accelerator," Nature Physics **2**, 696-699 (01 October 2006); Anthony Gonsalves et al., "Experimental Demonstration of 1 GeV Energy Gain in a Laser Wakefield Accelerator," Proc. of PAC07, Albuquerque, NM, June 25-29, pp. 1911-1915 (2007).